Submitted: 23 October, 2022 Accepted: 08 December, 2022 Published: 15 April, 2024 DOI:10.22514/ejgo.2024.031

ORIGINAL RESEARCH

European Journal of Gynaecological Oncology

A novel pyroptosis-related gene signature for predicting the prognosis of cervical cancer

Dan Li[1,2,3,†], Zhihua Du[4,†], Hualin Song[1,2,3], Rongjuan Li[4], Changhui Han[4], Xiao Wang[4], Ke Wang[1,2,3], Jingtao Luo[2,3,5,*]

[1]Department of Gynecological Oncology, Tianjin Medical University Cancer Institute and Hospital, National Clinical Research Center for Cancer, 300060 Tianjin, China
[2]Key Laboratory of Cancer Prevention and Therapy, 300060 Tianjin, China
[3]Tianjin's Clinical Research Center for Cancer, 300060 Tianjin, China
[4]Department of Oncology, Affiliated Hospital of Hebei University of Traditional Chinese Medicine, Provincial Hospital of Traditional Chinese Medicine, 051000 Shijiazhuang, Hebei, China
[5]Department of Maxillofacial and Otorhinolaryngology Oncology and Department of Head and Neck Oncology, Tianjin Medical University Cancer Institute and Hospital, 300060 Tianjin, China

***Correspondence**
jluo@tmu.edu.cn
(Jingtao Luo)

† These authors contributed equally.

Abstract

Although morbidity has decreased in developed regions, cervical cancer (CC) continues to have the highest incidence of all gynecological malignancies. The burden of morbidity and mortality in developing regions is also rising quickly, especially for advanced CC. Along with apoptosis, iron death, and other forms of programmed cell death, pyroptosis is a significant inflammatory process. Its connection to the malignancy mechanism has been verified. The expression of genes linked to pyroptosis in CC tissue and its relationship to prognosis, however, remain poorly understood. Using The Cancer Genome Atlas, we first discovered 13 differentially expressed pyroptosis-related genes (DE-PRGs) in the study (TCGA). Based on DE-PRGs, CC patients were divided into four subtypes. The 4 parts' times showed large variations according to the K-M curve. Then, using the least absolute shrinkage and selection operator (LASSO) Cox regression method, we created a mod el for predicting CC based on pyroptosis-associated genes. There were significant differences in overall survival (OS) times involving the high-risk and low-risk groups for all CC patients in the TCGA group, who were divided into low-risk and high-risk groups (p equals 0.0441). The risk score status as an independent prognostic factor for CC was confirmed by independent prognostic predictor validation. The analyses of single-sample gene set and enrichment analysis (ssGSEA), Kyoto Encyclopedia of Genes and Genomes (KEGG), and Gene Ontology (GO) all revealed significant differences in immune cells and immune pathways involving high- and low-risk groups (p less than 0.001), indicating a weakened immune status in high-risk groups. In conclusion, pyroptosis-associated genes are involved in tumor immunity and can help determine a patient's prognosis for CC. As a result, we have created and validated a signature that is related to pyroptosis and predicts CC prognosis, which may aid in early diagnosis, prognostic analysis, and immunotherapy.

Keywords

Cervical cancer; Pyroptosis; Prognosis; Signature; Bioinformatics; TCGA

1. Introduction

With an estimated 604,000 new cases and 342,000 fatalities worldwide in 2020 [1], cervical cancer (CC) ranks first in the incidence of gynecological malignant tumors and fourth in the incidence and mortality of malignant tumors in women. The 5-year relative survival rate for loco-regionally advanced CC is 58%, and the rate for distant disease is 17% [2]. Women who fall under the ages of 35 and 44 are most likely to develop CC, with an average age of 50 at diagnosis [3]. The primary cause of CC is high-risk human papillomavirus (HPV) infection. Although the HPV vaccine and early screening have decreased the incidence in Western countries, CC remains the leading cause of cancer-related deaths among women in developing countries due to socioeconomic conditions, particularly in most of Africa and Asia [4]. The two main forms of treatment for patients with metastatic or recurrent cervical cancer are chemotherapy and immunotherapy. The primary method for assessing the prognostic risk of CC at this time is still Federation International of Gynecology and Obstetrics (FIGO) staging, and due to the significant heterogeneity, a prediction model based on precise molecular markers is urgently required [5]. To prevent metastasis or recurrence, promptly alter treatment plans, increase survival rates, and lower mortality rates, it is essential to accurately identify high-risk patients. As a result, it is important to identify trustworthy biomarkers and create novice CC prognostic models.

The gasdermin (GSDM) protein family mediates pyroptosis, a type of inflammation that results in programmed cell death. At the moment, more research is being done on both classical pathways that depend on caspase-1 and nonclassical pathways that depend on caspase-4/5/11. Cell enlargement, plasma membranelysis, chromatin fragmentation, and the release of intracellular pro-inflammatory components are all effects of

pyroptosis. Pyroptosis significantly influences the growth, invasion, and metastasis of tumor cells, which has an impact on the course and prognosis of cancer [6]. Predictive models of pyroptosis-associated genes (PRGs) in ovarian cancer [7], lung adenocarcinoma [8], and glioma [9] have recently been established by a number of studies. The prognostic, diagnostic, and therapeutic value of pyroptosis in CC, however, is only briefly discussed in the literature, and it is unclear how PRGs function in CC.

In this study, we investigated the levels of PRG expression in CC using gene expression data from The Cancer Genome Atlas (TCGA) database, and CC patients were grouped according to PRG and clinical characteristics. We developed a prognostic model based on PRGs and assessed the sensitivity and specificity of the model. The analysis of functional and pathway enrichment, as well as the impact of prognosis-associated genes on immune pathways and tumor immune infiltration, were finally finished. By developing a new model of CC prognosis, our research data offers new biomarkers and targets for the diagnosis and treatment of CC.

2. Materials and methods

2.1 Datasets

On 01 September 2021, we collected 3 samples from healthy humans and 306 samples from patients with cervical cancer from the TCGA database [10] (https://portal.gdc.cancer.gov/repository). RNA sequences (RNA-seq) and the clinical features they are associated with, such as age, sex, survival status, and tumor grade, are found in bioinformatics and clinical data. The TCGA database's access guidelines and publication guidelines were strictly followed in this study.

2.2 Determination of pyroptosis-related genes with differential expression

From previously located literature, 33 genes related to pyroptosis were found [7]. R software (version 4.0.5, formerly AT&T, now Lucent Technologies, New Jersey, US) was the tool that was used the most throughout the entire research process. Gene expression values were uniformly normalized to fragment per kilobase million for differential gene expression analysis (FPKM). We conducted a consensus cluster analysis of 306 CC patients. We increase the consensus matrix K between 2 and 10. The appropriate K value was selected to analyze the prognosis. Using the "limma" package, we examined the DE-PRGs in 306 CC tissues and 3 normal tissues. DE-PRGs were defined as |log fold change| (|logFC|) > 0.5 and False positive rate (FDR) 0.05. A heat map of the outcomes was displayed. In addition, String (http://string-db.org) was used to visualize the protein-protein interaction (PPI) network of DE-PRGs (version 11.0).

2.3 Development of the pyroptosis-associated gene model for cervical cancer prediction

A model of CC risk prognosis based on DE-PRGs was required to further assess the significance of DE-PRGs in patients with poor prognoses for cervical cancer. In order to control system deviation, we first performed an analysis of Cox regressions with univariate variables to screen DE-PRGs related to OS. Adjusted p values were then presented in the assessment of the correlation involving DE-PRGs and OS. Five DE-PRGs were recognized as risk genes for the predictive model under the screening criteria of p less than 0.05. A prognostic model and risk scoring formula based on 5 genes were then presented, and LASSO regression by the "glmnet" package was established to prevent model overfitting. Following this, 306 CC patients were divided into low- and high-risk groups based on the median risk score, and Kaplan-Meier analysis was used to compare the difference in OS time between the two groups. On the basis of the 5 genes, we used the "stats" package for principal component analysis. Finally, using the "survival", "survminer", and "timeROC" packages, receiver operating characteristic (ROC) curve analysis at 1, 2, and 3 years was performed.

2.4 Independent prognostic predictor validation

We used age, tumor grade, and the risk score as three covariates in univariate and multivariate Cox regression analyses to test whether the risk score was a standalone prognostic factor for overall survival (OS) in CC patients.

2.5 Analysis of functional and pathway enrichment

To research the DE-PRGs' biomedical molecular mechanism. The "clusterProfiler" package was used to conduct analyses of the Gene Ontology (GO) and Kyoto Encyclopedia of Genes and Genomes (KEGG). Statistics were deemed significant at p less than 0.05.

2.6 Evaluation of the prognostic signature of infiltrating immune cells

Using the "gsva" package, single-sample gene set enrichment analysis (ssGSEA) was used to evaluate the different immune cell types' levels of infiltration, immune-related functions, and immune-associated pathways in various risk subgroups.

2.7 Statistical investigation

R software was used to complete all of the statistical analyses for this study. The first step was to compare the differentially expressed genes in normal tissues and CC tissues using univariate analysis of variance (ANOVA) and the chi-squared (2) test. Then, using Kaplan-Meier survival curves and the log-rank test, the OS of the four subgroups was compared. Independent validation of the risk prediction model was carried out using both univariate and multivariate regression analyses. In order to compare the enrichment values of immune cells and immune pathways involving subgroups, we used the Mann-Whitney U test. In Fig. 1, the flow chart was displayed.

3. Outcomes

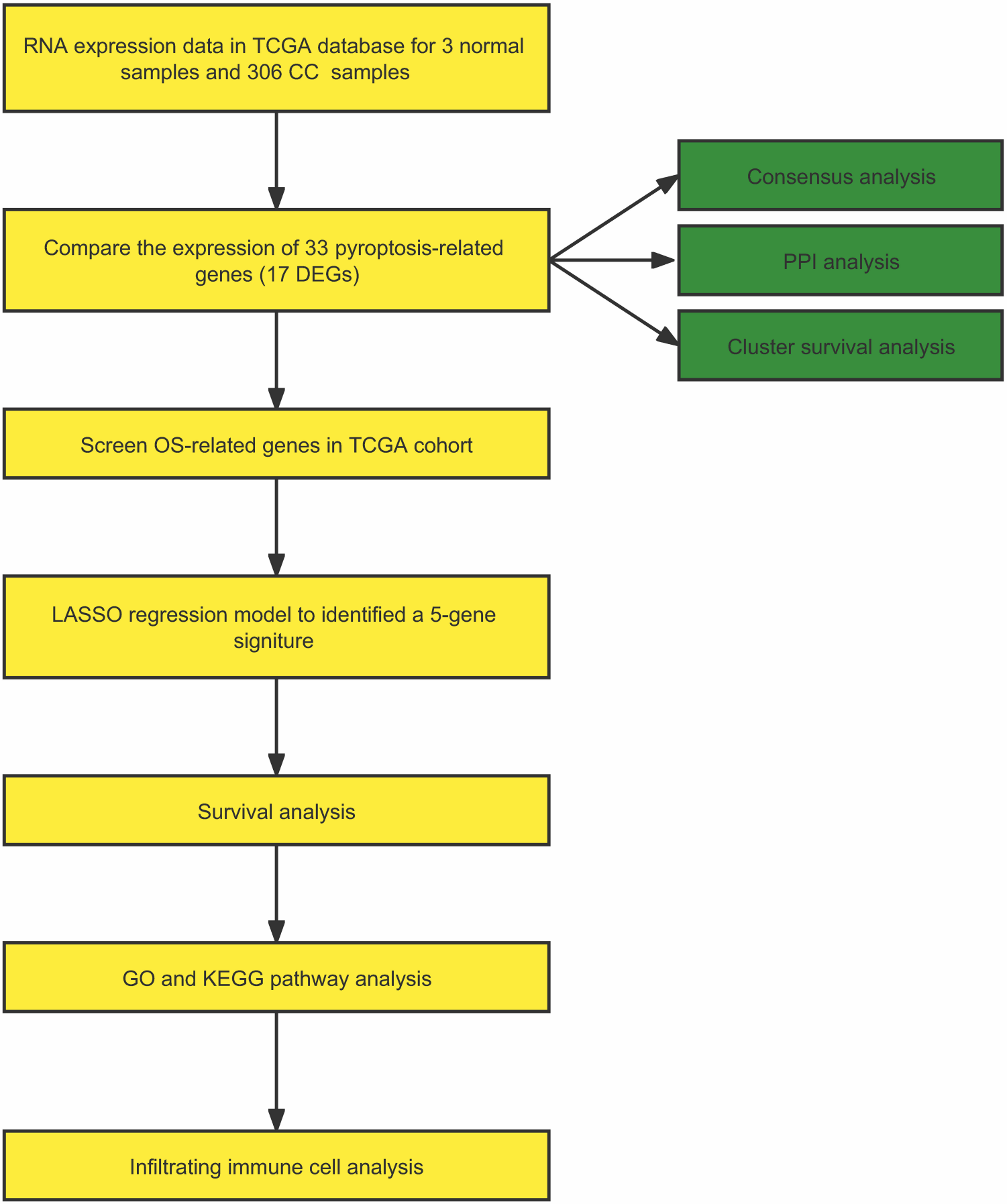

FIGURE 1. The specified workflow picture of information dissection. TCGA: The Cancer Genome Atlas; CC: cervical cancer; GO: Gene Ontology; KEGG: Kyoto Encyclopedia of Genes and Genomes; PPI: protein-protein interaction; DEGs: differentially expressed genes; OS: overall survival; LASSO: least absolute shrinkage and selection operator.

TABLE 1. The expression of PRGs between normal samples and cervical cancer tissues.

gene	logFC	*p*
GSDMC	7.862221	0.003662
GSDMB	3.112795	0.004590
NOD2	3.427569	0.004977
CASP3	1.190806	0.008141
NLRP7	8.936591	0.008957
PYCARD	2.146169	0.010222
TNF	3.456196	0.010811
IL18	2.799112	0.011220
CASP6	1.089384	0.011430
AIM2	6.218314	0.013480
CASP8	1.238229	0.015293
CASP5	3.489072	0.017623
ELANE	−2.909690	0.017991
NLRP1	−1.223890	0.023634
CASP4	1.068867	0.032911
NOD1	−0.591720	0.037414
NLRP2	5.075027	0.039856
PJVK	−0.712440	0.055001
CASP1	1.369288	0.076807
SCAF11	0.444498	0.087067
GSDMA	2.724424	0.123013
IL1B	1.809181	0.129452
GSDME	−0.466370	0.139594
TIRAP	−0.602210	0.150337
NLRP3	−0.544070	0.223392
CASP9	−0.202770	0.285428
NLRC4	0.545963	0.297305
GSDMD	0.421161	0.325220
NLRP6	0.760673	0.359875
PLCG1	−0.121860	0.396761
PRKACA	−0.127110	0.415100
GPX4	0.441223	0.493294
IL6	−1.215250	0.888966

FC: fold change; P: p-value; GSDM: Gasdermin; NOD: Nucleotide Binding Oligomerization Domain Containing; CASP: Caspase; NLRP: NLR Family Pyrin Domain Containing; PYCARD: PYD And CARD Domain Containing; TNF: Tumor Necrosis Factor; IL: Interleukin; AIM: Absent In Melanoma; ELANE: Elastase Neutrophil Expressed; PJVK: Pejvakin; SCAF: SR-Related CTD Associated Factor; TIRAP: TIR Domain Containing Adaptor Protein; PLCG: Phospholipase C Gamma; PRKACA: Protein Kinase CAMP-Activated Catalytic Subunit Alpha; GPX: Glutathione Peroxidase.

3.1 DE-PRG identification using normal samples as well as cervical cancer tissues

To begin with, we compared the expression levels of 33 PRGs in 3 normal samples and 306 CC tissues and rendered them as a heatmap in Fig. 2A (green indicates a low level of expression; red indicates a high level of expression). Among them, 22 genes (*Absent In Melanoma 2* (*AIM2*), *Caspase 1* (*CASP1*), *CASP3*, *CASP4*, *CASP5*, *CASP6*, *CASP8*, *Glutathione Peroxidase 4* (*GPX4*), *Gasdermin A* (*GSDMA*), *GSDMB*, *GSDMC*, *GSDMD*, *Interleukin 18* (*IL18*), *IL1*, *NLR Family CARD Domain Containing 4* (*NLRC4*), *NLR Family Pyrin Domain Containing 2* (*NLRP2*), *NLRP6*, *NLRP7*, *Nucleotide Binding Oligomerization Domain Containing 2* (*NOD2*), *PYD And CARD Domain Containing* (*PYCARD*), *SR-Related CTD Associated Factor 11* (*SCAF11*), and *Tumor Necrosis Factor* (*TNF*)) showed high levels of expression. There were 11 genes with low expression (*CASP9*, *Elastase Neutrophil Expressed* (*ELANE*), *GSDME*, *IL6*, *NLRP1*, *NLRP3*, *NOD1*, *Pejvakin* (*PJVK*), *Phospholipase C Gamma 1* (*PLCG1*), *Protein Kinase CAMP-Activated Catalytic Subunit Alpha* (*PRKACA*), and *TIR Domain Containing Adaptor Protein* (*TIRAP*)). In addition, 17 genes were identified by p less than 0.05 (* if p less than 0.05, ** if p less than 0.01), of which 5 genes (*NLRP7*, *NOD2*, *CASP3*, *GSDMB*, and *GSDMC*) were distinctly different (p less than 0.01), while p less than 0.05 could not be determined for the remaining 12 genes (*NLRP2*, *CASP5*, *ELANE*, *NLRP1*, *NOD1*, *TNF*, *PYCARD*, *CASP6*, *CASP8*, *IL-18*, *CASP4*, as well as *AIM2*). The specific expression of PRGS is detailed in Table 1. Subsequently, the PPI plot (Fig. 2B) indicated various associations among 33 PRGs and hub genes, including *CASP1*, *CASP3*, *CASP5*, *CASP4*, *CASP8*, *CASP9*, *AIM2*, *NLRC4*, *IL18*, *IL1B*, *PYCARD*, *NOD2*, *NLRP1*, *NLRP3*, *GSDMD*, and *TNF*. All hub genes had p values less than 0.05, except for *CASP1*, *CASP9*, *NLRC4*, *IL1B*, *NLRP3*, and *GSDMD*. Moreover, we conducted a correlation network for all PRGs, which is shown in Fig. 2C (the color red indicates positive correlations and the color blue indicates negative correlations).

3.2 Cervical cancer subgroups on the basis of DE-PRGs

We chose ($|\log FC|$) $>$ 0.5 and FDR less than 0.05 as the criteria for screening DE-PRGs. We found 13 DE-PRGs (*AIM2*, *CASP3*, *CASP5*, *CASP6*, *CASP8*, *ELANE*, *GSDMB*, *GSDMC*, *IL18*, *NLRP7*, *NOD2*, *PYCARD*, *TNF*). To identify CC subtypes on the basis of 13 DE-PRGs, we conducted a consensus cluster analysis of 306 CC patients. We increase the consensus matrix K between 2 and 10, the result showing that when k = 4, the intragroup correlation is maximum, while the intergroup correlation is the lowest. Therefore, 306 CC patients can be categorized to 4 different subgroups on the basis of DE-PRGs. (Fig. 3A). As shown in the heat map (Fig. 3B), there were no significant differences involving the 4 subgroups regarding clinical and pathologic features, including age, sex, survival status, and tumor grade. However, which is very important, the K-M curve indicated considerable variations in os time involving the 4 subgroups (Fig. 3C, p equals 0.007).

3.3 Construction of the model for predicting cervical cancer by pyroptosis-associated genes

We conducted an analysis of Cox regressions with univariate variables to locate DE-PRGs associated with OS, and *TNF* were identified as risk genes for the dangerous model, with p less than 0.0001, hazard ratio (HR) equals 1.0828 (1.0471–1.1197) (Fig. 4A). Then, we found another 4 DE-PRGs with p values less than 0.4 (*AIM2*, *CASP5*, *NLRP7*, *PYCARD*) (Fig. 4A). We conducted multivariate Cox regression analysis among the 5 genes and identified 1 gene (*AIM2*) was protective, with p equals 0.0405, HR equals 0.9857 (0.9722–0.9994), and 2 genes (*CASP5* and *TNF*) were dangerous, with p equals 0.0419 and HR equals 1.3361 (1.0106–1.7663) and p less than 0.001, with HR equals 1.0906 (1.0544–1.1280) (Fig. 4B). By performing the LASSO Cox regression analysis, a 5-gene signature was constructed according to the optimum λ value (Fig. 4C,D). Thus, the risk scores of all patients could be calculated by the gene expression levels and invariant regression coefficients in the model. The formula for the prognostic risk assessment score was as follows: risk score = (-0.014431 $\times$ AIM2 exp.) plus (0.289740 $\times$ CASP5 exp.) plus (-0.011175 $\times$ NLRP7 exp.) plus (−0.012916 $\times$ PYCARD exp.) plus (0.086690 $\times$ TNF exp.). On the basis of the median risk score, 306 CC patients were categorized to low- and high-risk subgroups (Fig. 4E). The principal component analysis (PCA) revealed that patients were split into 2 clusters and that as the risk score rose, so did the risk of death and the duration of survival (Fig. 5A,B). High- and low-risk subgroups OS times were significantly different, according to the Kaplan-Meier curve (p equals 0.0441, Fig. 5C). Finally, the ROC curve, which represented the predictive performance, indicated that the areas under the ROC curve (AUCs) were 0.624, 0.686, and 0.678 at 1 year, 2 years, and 3 years, respectively (Fig. 5D).

3.4 Validation of independent prognostic predictor

The analysis of Cox regressions with univariate variables indicated that HR equals 1.7162, 95% confidence interval (CI) (1.0322–2.8534), p equals 0.0373, which demonstrated that the risk score was significantly correlated with OS time (Fig. 6A). Moreover, after further adjustment for confounding factors, multivariate Cox regression analysis proved that the risk score remains an independent prognostic factor for CC. (HR equals 1.7592, 95% CI (1.0459–2.9592), p equals 0.0332, Fig. 6B). Additionally, we created a heatmap of clinical characteristics for the TCGA group (Fig. 6C), and we discovered that the age of patients as well as their survival status varied widely across the low- and high-risk subgroups (p less than 0.05).

3.5 Functional enrichment and pathway analysis

To explore genetic function and pathway differences involving two risk subgroups on the basis of the risk predictive model, we completed functional and pathway enrichment analysis. Firstly, we extracted differentially expressed genes (DEGs) involving the two subgroups from the TCGA database by

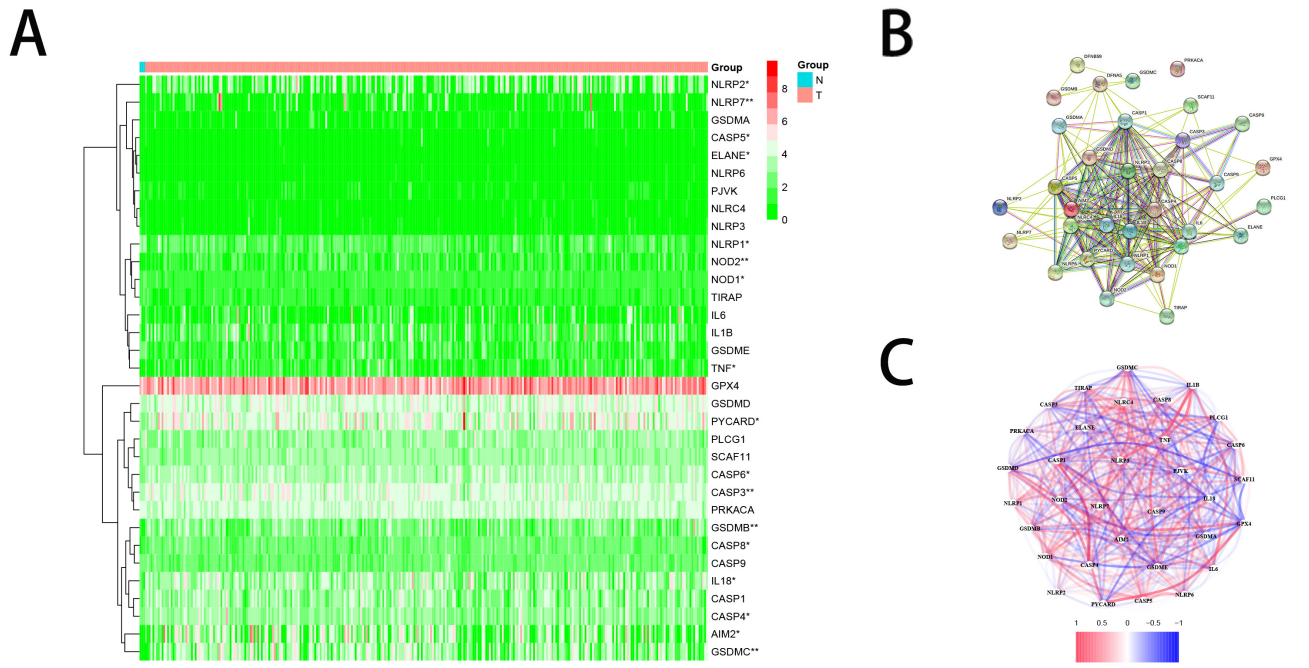

FIGURE 2. Identification of DE-PRGs involving normal samples and cervical cancer tissues. (A) Heatmap of the PRGs involving the normal and the tumor tissues. (B) PPI network showing the interactions of the PRGs. (C) The correlation network of the PRGs (red line: positive correlation; blue line: negative correlation. The depth of the colors reflects the strength of the relevance). *p* values were indicated as: **p* less than 0.01, ***p* less than 0.01, ****p* less than 0.001. DE-PRGs: differentially expressed pyroptosis-related genes; PRGs: pyroptosis-related genes; PPI: protein-protein interaction.

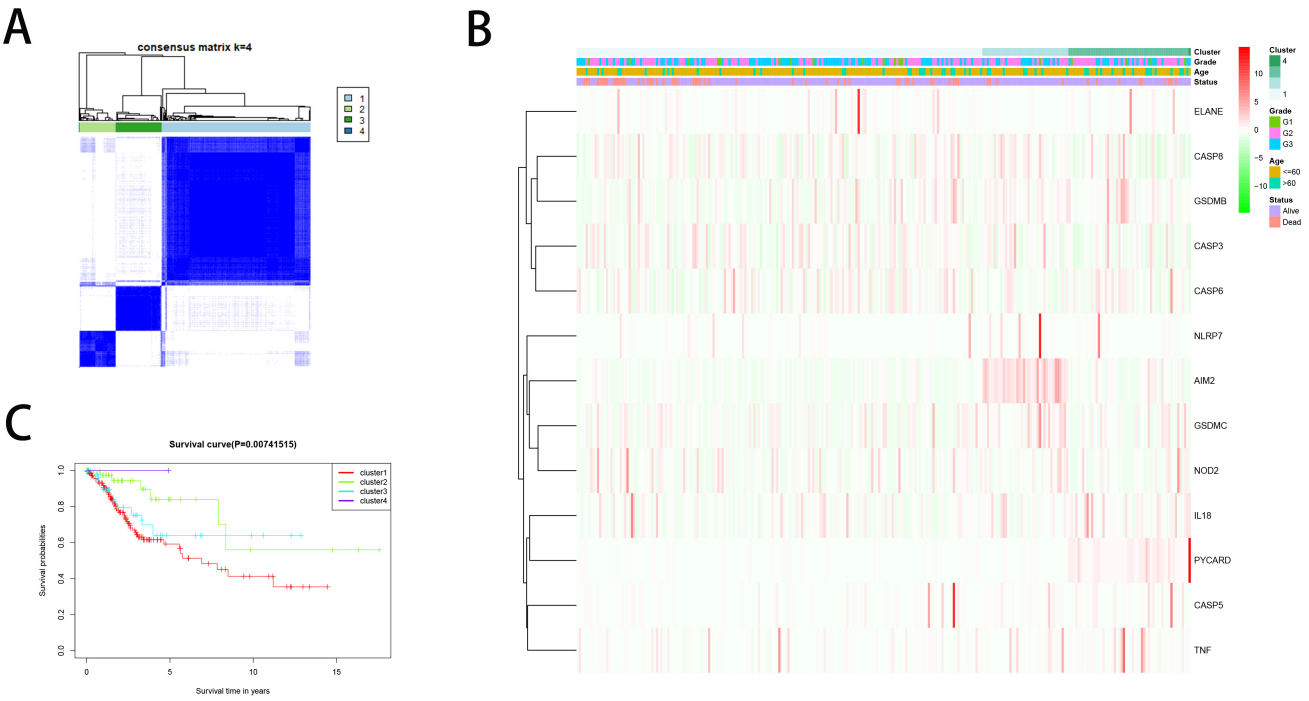

FIGURE 3. Cervical cancer subgroups on the basis of DE-PRGs. (A) 306 CC patients were grouped into four clusters according to the consensus clustering matrix (k = 4). (B) Heatmap and the clinicopathologic characters of the two clusters classified by these DE-PRGs. (C) Kaplan-Meier OS curves for the four clusters.

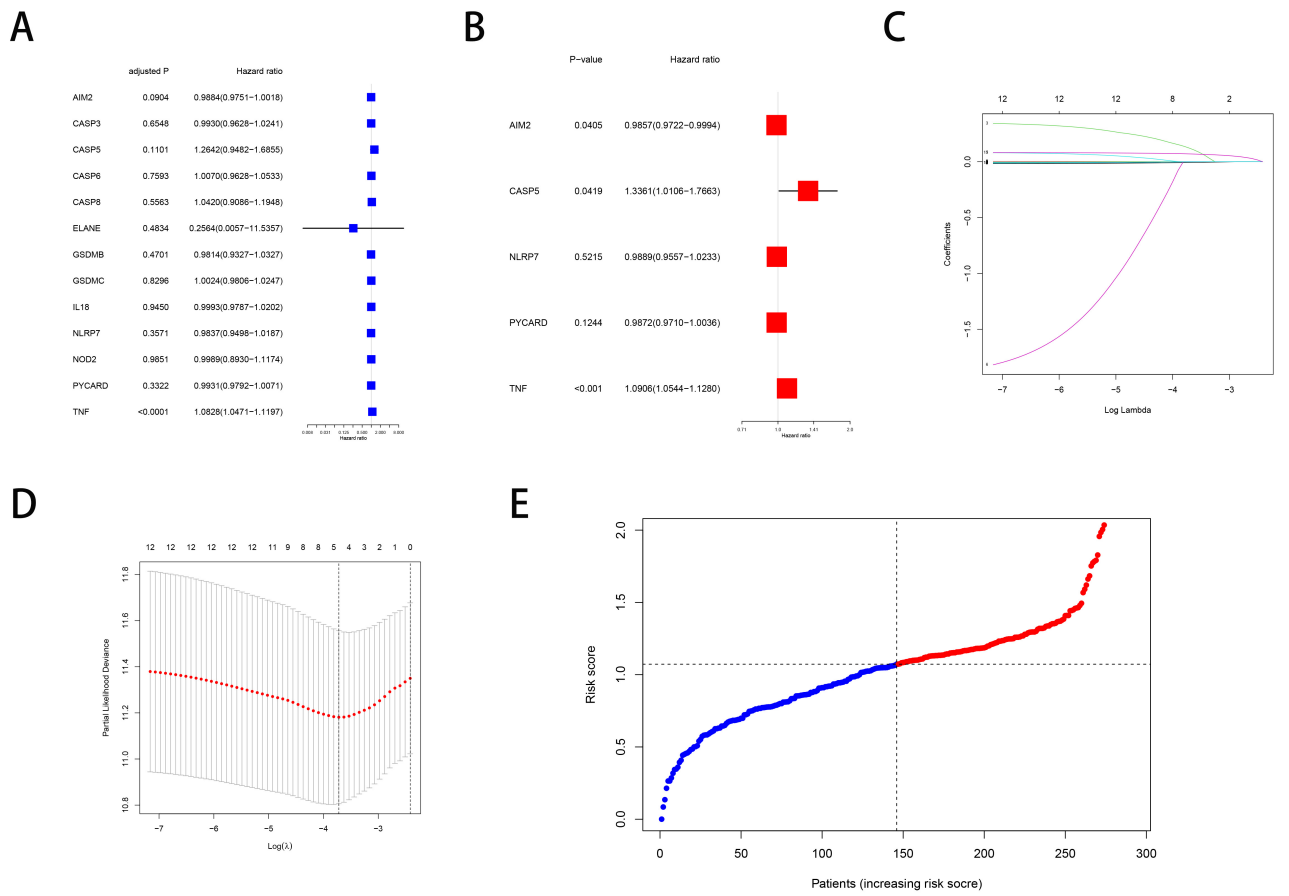

FIGURE 4. Construction of the risk model by DE-PRGs. (A) an analysis of cox regressions with univariate variables of OS for each DE-PRGs. (B) Multivariate Cox regression analysis among the 5 genes (*TNF*, *AIM2*, *CASP5*, *NLRP7*, *PYCARD*). (C,D) LASSO regression of the DE-PRGs. (E) Distribution of patients on the basis of the risk score.

the "limma" package (FDR less than 0.05 and $|\log2FC| \geq 1$). Thus, 709 DEGs were exposed. Then, using DEGs as a base, functional and pathway analysis were carried out. According to GO functional enrichment analysis, DEGs were primarily enriched in five biological process (BP) aspects: synapse organization, cell-cell adhesion *via* plasma-membrane adhesion molecules, extracellular matrix organization, and extracellular structure organization. DEGs were significantly enriched in two aspects of molecular function (MF), namely, receptor ligand activity and signaling receptor activator activity. Regarding the cellular component (CC), the synaptic membrane, glutamatergic synapse, neuron to neuron synapse, and postsynaptic membrane were the four areas where DEGs were most enriched (Fig. 7A). Later, KEGG pathway enrichment analysis revealed that DEGs were significantly enriched in the following pathways, including the calcium signaling pathway, cytokine-cytokine receptor interaction, and neuroactive ligand-receptor (Fig. 7B). This finding suggests that DEGs may be connected to cellular interactions as well as immune-related interactions.

3.6 Infiltrating immune cell assessment of the prognostic signature

Using ssGSEA, we thoroughly compared the differences between the low- or high-risk subgroups for 16 different immune cell types and 13 immune pathways. Interestingly, the box diagram showed that 14 immune cell types in the low-risk group were greater than those in the high-risk group, with the exception of mast cells and neutrophils. They included a Dendritic cells (aDCs), cluster of differentiation 8+ (CD8+) T cells, natural killer (NK) cells, plasmacytoid dendritic cells, follicular helper T cells (Tfh), Th1 cells, Th2 cells, and tumour-infiltrating lymphocytes (TIL), all of which were significantly higher than the high-risk group (Fig. 8A, p less than 0.001). In addition, the enrichment values of the low-risk group in the other 12 immune pathways—particularly APC co-stimulatory, checkpoint, cytolytic activity, inflammation-promoting, major histocompatibility complex (MHC) class I, parainflammatory, T-cell co-inhibitory, T cell co-stimulation, and Type I interferon (IFN) response—were generally higher than those of the high-risk group (Fig. 8B, p less than 0.001).

4. Discussion

In recent decades, pyroptosis has contributed significantly to programmed death of cells, which has received more and more attention, and many associated studies are also underway. Pyroptosis has a two-way impact on occurrence and progression of cancer. Pyroptosis releases inflammatory factors that cause normal cell mutations, and immune cells pyroptosis can also

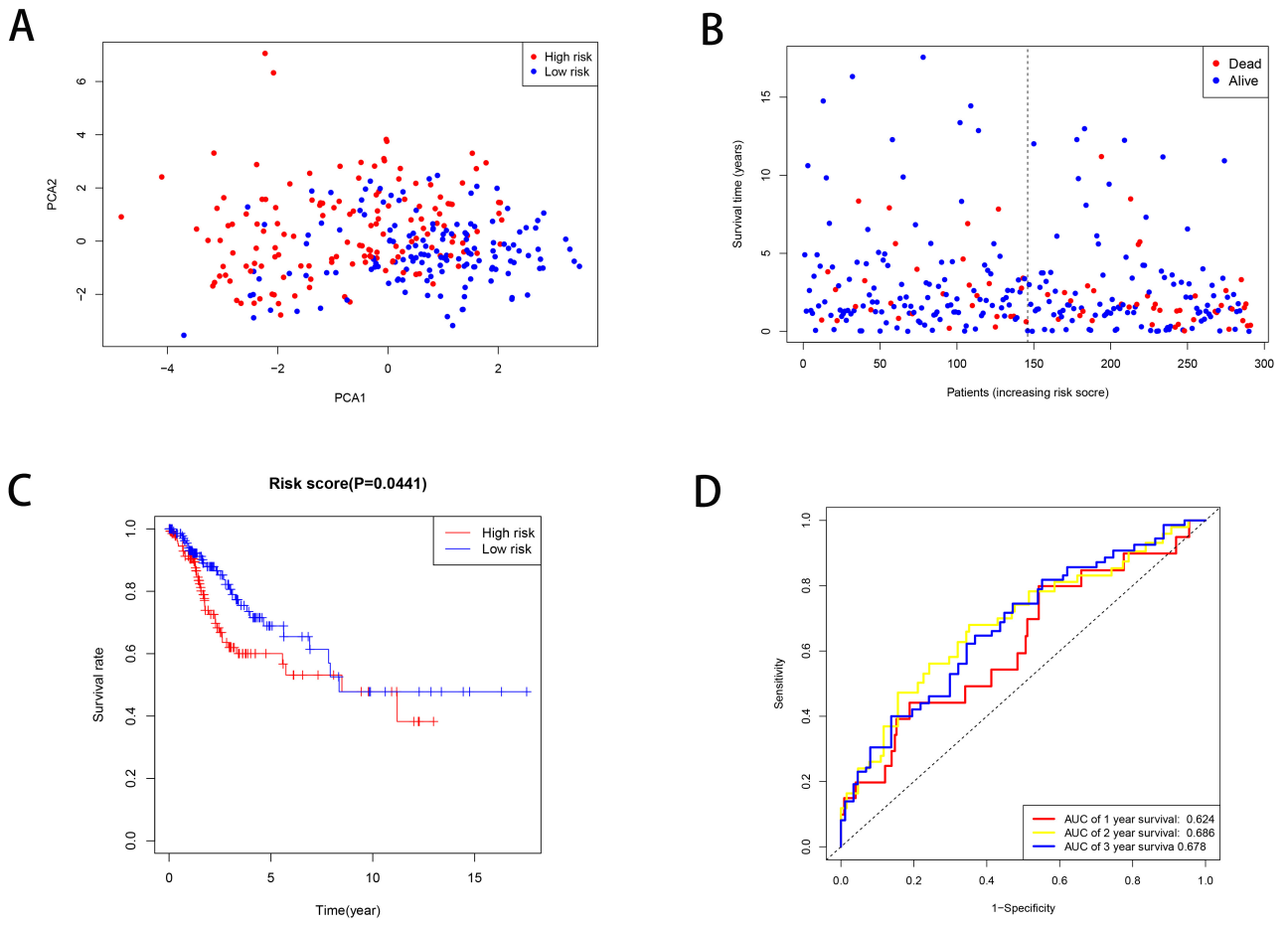

FIGURE 5. The risk signature for predicting the prognosis of cervical cancer. (A) PCA plot for CCs on the basis of the risk score. (B) The survival status for each patient. (C) Kaplan-Meier curves for the OS of patients. (D) ROC curves demonstrated the predictive efficiency of the risk score. AUC: areas under the curve; PCA: principal component analysis.

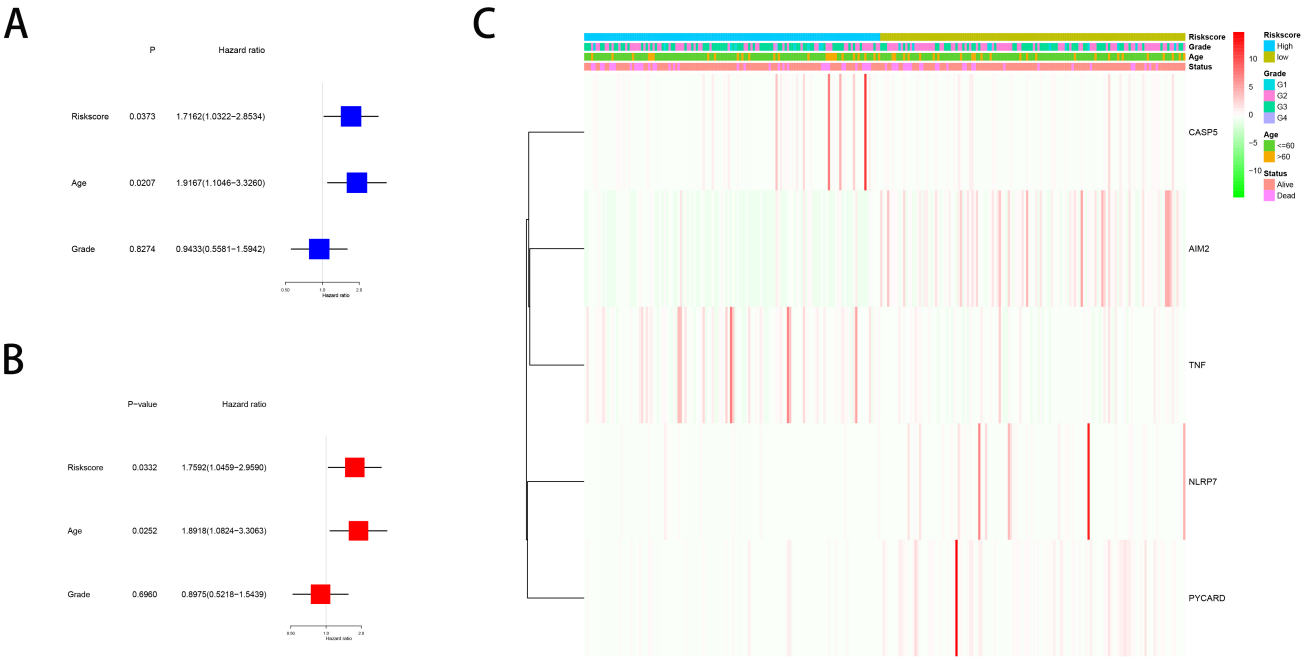

FIGURE 6. Validation of independent prognostic predictor. (A) Univariate analysis for the TCGA group. (B) Multivariate analysis for the TCGA group. (C) Heatmap involving clinicopathologic features and the risk groups.

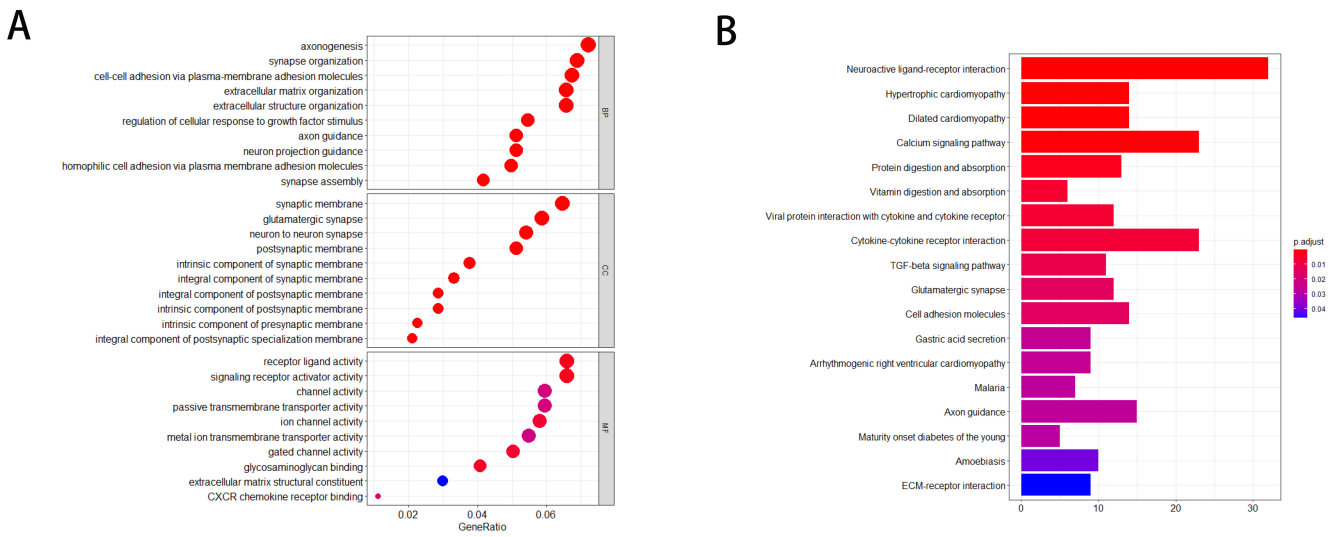

FIGURE 7. Functional enrichment and pathway analysis. (A) Bubble graph for GO enrichment. (B) Barplot graph for KEGG pathways. TGF: Transforming Growth Factor; ECM: Extracellular matrix.

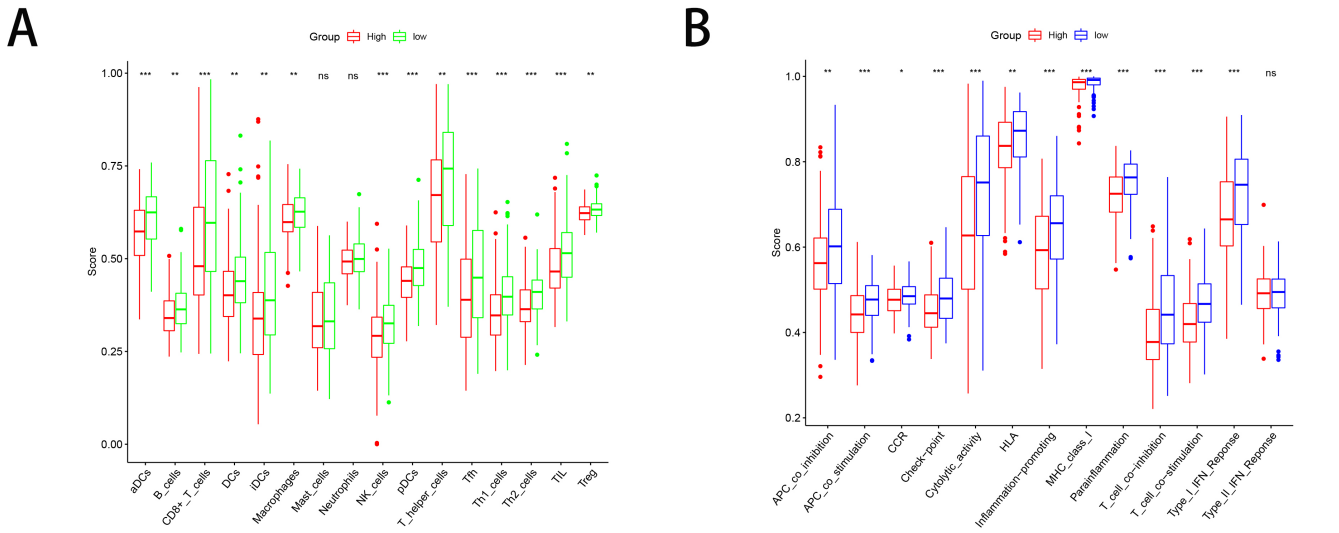

FIGURE 8. Infiltrating immune cell assessment of the prognostic signature. (A) Comparison of the enrichment values of 16 types of immune cells involving low- and high-risk group in the TCGA group. (B) Comparison of the enrichment values of 13 immune-associated pathways involving low- and high-risk group in the TCGA group.

trigger tumorigenesis. Conversely, tumor cells pyroptosis will suppress cancer progression [11, 12]. Therefore, inhibiting normal cells pyroptosis, but promoting tumor cells could be an important direction for cancer prevention and treatment. Predictive models of pyroptosis-associated genes have established in several cancers, including ovarian cancer [7], lung adenocarcinoma [13], gastric cancer [14] and glioma [9]. Zhou *et al.* [15] screened 8 pyroptosis-associated genes (*GPX4*, *GSDME*, Granzyme A (*GZMA*), *GZMB*, *IL1B*, *NOD1*, *PRKACA*, *TNF*) associated with CC prognosis, but the pyroptosis as a predictive marker for cancer of the colon is still not fully elucidated.

In this study, we first examined 33 known PRG mutations and variants in CC samples and discovered that the majority were highly expressed. We then used PPI analysis to confirm the association of 33 PRGs. In order to thoroughly evaluate the prognostic value of these pyroptosis-related regulators, we used consensus clustering to separate the CC samples into four subgroups based on the DE-PRGs. The 4 groups of CC subgroups showed significant differences in survival analyses. By using multivariate Cox analysis and lasso analysis, we created a CC prognosis model that contains 5 PRGs. The risk score was inversely correlated with immune cell infiltration of T cells, NK cells, B cells, dendritic cells, and macrophages, according to ssGSEA analysis, which also showed that immune cell infiltration has a significant impact on the survival of CC patients.

The prognostic model of CC established in this research

suggests that *CASP55* and *TNF* are biomarkers of poor prognosis, while *AIM2*, *NLRP7*, and *PYCARD* are indeed protective. *AIM2*, as the main regulator of pyroptosis, initiates the intrinsic immunity of cells by activating Caspase-1, followed by shearing pro-IL-1β and pro-IL-18. *AIM2* deficiency is linked to a poor prognosis for prostate cancer [16], colon cancer [17], and breast cancer [18], according to research, which has demonstrated that *AIM2* has the opposite effect in various cancers. However, lung adenocarcinoma [19, 20], gastric cancer [21], and cutaneous squamous cell carcinoma [22] all have poor prognoses when *AIM2* is highly expressed. So *et al*. [23] reported that Sirtuin 1 (SIRT1) knock-down cells induced CC cell pyroptosis by activating more *AIM2* inflammasomes. Hsu *et al*. [24] discovered that high expression of *AIM2* was positively correlated with antiangiogenic drugs resistance in epithelial ovarian cancer.

A member of the NLR family known as *NLRP7* (nucleotide-binding domain and leucine-rich repeat-containing family, pyrin domain-containing 7) is thought to play a role in inflammation and innate immunity [25]. In a genetic reconstitution study using the human embryonic kidney (HEK) 293 cell line, *NLRP7* was discovered to inhibit caspase-1-mediated IL-1β maturation, indicating an anti-inflammatory function [26]. Li *et al*. [27] proved that high expression of *NLRP7* in colorectal cancer (CRC) could promote tumor progression. According to Ohno *et al*. [28], endometrial cancer patients with high *NLRP7* expression had a poor prognosis and a higher risk of myometrial invasion. According to another study, *NLRP7* directly contributes to the development of choriocarcinomas and suppresses the immune system, which aids in the spread of the tumor [29]. However, in contrast to earlier research, our study showed that *NLRP7* was a protective factor.

Activating signal cointegrator (ASC), a crucial adapter protein that assembles and activates through homologous interactions, is encoded by the gene *PYCARD*. It is an intracellular signaling molecule made up of the pyrin domain (PYD) at the N-terminus and the caspase recruitment domain (CARD) at the C-terminus [30]. A frequent and early occurrence in the development of many tumors, including ovarian cancer [31], prostate cancer [32], non-small cell lung cancer [29], and breast cancer [33], is abnormal hypermethylation of the *PYCARD* promoter region. These studies suggested that *PYCARD* might function as a tumor suppressor gene and that its silencing might increase the risk of developing particular tumors. The finding that *PYCARD* is a protective factor in CC prognosis presented in our study is consistent with this finding. Despite this, Liang *et al*. [34] demonstrated that high *PYCARD* expression is a standalone predictor of a poor prognosis as well as chemotherapy resistance throughout glioma.

Caspase 5 contributes significantly to both classical and nonclassical inflammasome-induced pyroptosis. Caspase 5 is activated when the pattern-recognition receptors recognize cytoplasmic lipopolysaccharide, which in turn cleave gasdermin-D (GSDMD), releasing inflammatory factors that lead to pyroptosis. This is when caspase 5 is activated. On the other hand, Caspase 5 that has been activated can interact with Caspase 1 to encourage its activation and cause pyroptosis *via* the traditional pathway. Caspase 5 has been linked to the development and prognosis of several cancers, including gastric cancer [35], glioblastoma polymorphic [36], cervical cancer [37], and osteosarcoma [38]. According to Zhou *et al*.'s findings, l ong-non-coding RNA Caspase 5 promoted the malignant phenotypes of human glioblastoma multiforme [36]. Zhang *et al*. [38] proposed that Caspase 5 is associate with poor prognosis in the pyroptosis related model of osteosarcoma. Babas *et al*. [37] found that serum caspase-5 activity was elevated in patients with CC, which indicating that Caspase 5 could be involved in the cervical malignancy mechanisms.

T lymphocytes, macrophages, and NK cells all produce *TNF*, an inflammatory substance. Apoptosis and pyroptosis are triggered by the activation of *TNF*- and its involvement in the formation of *NLRP3* inflammasomes, which are mediated by Caspase 1. According to Sha *et al*. [39], serum levels of *TNF*- in CC patients were noticeably elevated before surgical intervention, and they then went back to normal. A genetic variant of the *TNF*-α gene (rs1800629) was linked to higher levels and risks of developing CC, according to research by Behboodi *et al*. [40].

Our current study had a number of drawbacks. First off, the sample size was relatively small, the original data was only retrieved from the TCGA database, and there was no external database validation or support for large sample sizes. Second, we were unable to perform a more thorough clinical analysis because we lacked information on the samples' clinical characteristics. Third, further investigation and translational therapy through clinical and experimental studies are required. The molecular mechanism underlying the impact of pyroptosis on patients with CC prognosis is unknown.

5. Conclusions

To summarize, our study used the public database TCGA to construct a CC prediction model using R language and statistical analysis based on five genes associated with pyroptosis. Using this model, one may be able to accurately predict the prognosis of CC, provide a new strategy for exploring the molecular markers and pathogenesis of CC, and establish an important reference for future molecular precision treatment of CC.

ABBREVIATIONS

CC: Cervical cancer; DE-PRGs: Differentially expressed pyroptosis-associated genes; GSDM: gasdermin; Lasso: Least absolute shrinkage & selection operator; NLRP7: Nucleotide-binding domain and leucine-rich repeat-containing family, pyrin domain-containing 7; PRGs: Pyroptosis-associated genes; ROC: Receiver operating characteristic; ssGSEA: Single sample gene set enrichment analysis; TCGA: The Cancer Genome Atlas.

AVAILABILITY OF DATA AND MATERIALS

The data presented in this study are available on reasonable request from the corresponding author.

AUTHOR CONTRIBUTIONS

JTL and KW—designed the research study. DL—performed the research. HLS, RJL and CHH—analyzed the data. HLS and XW—wrote the manuscript. All authors read and approved the final manuscript.

ETHICS APPROVAL AND CONSENT TO PARTICIPATE

Not applicable.

ACKNOWLEDGMENT

We are grateful for the data provided by the TCGA database.

FUNDING

This research was funded by National Natural Science Foundation of China, grant number 82073006.

CONFLICT OF INTEREST

The authors declare no conflict of interest.

REFERENCES

[1] Sung H, Ferlay J, Siegel RL, Laversanne M, Soerjomataram I, Jemal A, *et al*. Global cancer statistics 2020: GLOBOCAN estimates of incidence and mortality worldwide for 36 cancers in 185 countries. CA: A Cancer Journal for Clinicians. 2021; 71: 209–249.

[2] Brodeur MN, Dejean R, Beauchemin MC, Samouëlian V, Cormier B, Bacha OM, *et al*. Oncologic outcomes in the era of modern radiation therapy using FIGO 2018 staging system for cervical cancer. Gynecologic Oncology. 2021; 162: 277–283.

[3] American Cancer Society. About cervical cancer. 2022. Available at: https://www.cancer.org/cancer/cervical-cancer/about/what-is-cervical-cancer.html (Accessed: 25 January 2022).

[4] Buskwofie A, David-West G, Clare CA. A review of cervical cancer: incidence and disparities. Journal of the National Medical Association. 2020; 112: 229–232.

[5] Chen H, Deng Q, Wang W, Tao H, Gao Y. Identification of an autophagy-related gene signature for survival prediction in patients with cervical cancer. Journal of Ovarian Research. 2020; 13: 131.

[6] Fang Y, Tian S, Pan Y, Li W, Wang Q, Tang Y, *et al*. Pyroptosis: a new frontier in cancer. Biomedicine & Pharmacotherapy. 2020; 121: 109595.

[7] Ye Y, Dai Q, Qi H. A novel defined pyroptosis-related gene signature for predicting the prognosis of ovarian cancer. Cell Death Discovery. 2021; 7: 71.

[8] Lin W, Chen Y, Wu B, Chen Y, Li Z. Identification of the pyroptosisrelated prognostic gene signature and the associated regulation axis in lung adenocarcinoma. Cell Death Discovery. 2021; 7: 161.

[9] Chao B, Jiang F, Bai H, Meng P, Wang L, Wang F. Predicting the prognosis of glioma by pyroptosis-related signature. Journal of Cellular and Molecular Medicine. 2022; 26: 133–143.

[10] Liu J, Lichtenberg T, Hoadley KA, Poisson LM, Lazar AJ, Cherniack AD, *et al*. An integrated TCGA pan-cancer clinical data resource to drive high-quality survival outcome analytics. Cell. 2018; 173: 400–416.e11.

[11] Ruan J, Wang S, Wang J. Mechanism and regulation of pyroptosis-mediated in cancer cell death. Chemico-Biological Interactions. 2020; 323: 109052.

[12] Zheng Z, Li G. Mechanisms and therapeutic regulation of pyroptosis in inflammatory diseases and cancer. International Journal of Molecular Sciences. 2020; 21: 1456.

[13] Song J, Sun Y, Cao H, Liu Z, Xi L, Dong C, *et al*. A novel pyroptosis-related lncRNA signature for prognostic prediction in patients with lung adenocarcinoma. Bioengineered. 2021; 12: 5932–5949.

[14] Shao W, Yang Z, Fu Y, Zheng L, Liu F, Chai L, *et al*. The Pyroptosis-related signature predicts prognosis and indicates immune microenvironment infiltration in gastric cancer. Frontiers in Cell and Developmental Biology. 2021; 9: 676485.

[15] Zhou C, Li C, Zheng Y, Liu X. Identification of pyroptosis-related signature for cervical cancer predicting prognosis. Aging. 2021; 13: 24795–24814.

[16] Ponomareva L, Liu H, Duan X, Dickerson E, Shen H, Panchanathan R, *et al*. AIM2, an IFN-inducible cytosolic DNA sensor, in the development of benign prostate hyperplasia and prostate cancer. Molecular Cancer Research. 2013; 11: 1193–1202.

[17] Dihlmann S, Tao S, Echterdiek F, Herpel E, Jansen L, Chang-Claude J, *et al*. Lack of absent in melanoma 2 (AIM2) expression in tumor cells is closely associated with poor survival in colorectal cancer patients. International Journal of Cancer. 2014; 135: 2387–2396.

[18] Chen IF, Ou-Yang F, Hung JY, Liu JC, Wang H, Wang SC, *et al*. AIM2 suppresses human breast cancer cell proliferation *in vitro* and mammary tumor growth in a mouse model. Molecular Cancer Therapeutics. 2006; 5: 1–7.

[19] Colarusso C, Terlizzi M, Lamort A, Cerqua I, Roviezzo F, Stathopoulos G, *et al*. Caspase-11 and AIM2 inflammasome are involved in smoking-induced COPD and lung adenocarcinoma. Oncotarget. 2021; 12: 1057–1071.

[20] Zhang M, Jin C, Yang Y, Wang K, Zhou Y, Zhou Y, *et al*. AIM2 promotes non-small-cell lung cancer cell growth through inflammasome-dependent pathway. Journal of Cellular Physiology. 2019; 234: 20161–20173.

[21] Dawson RE, Deswaerte V, West AC, Tang K, West AJ, Balic JJ, *et al*. STAT3-mediated upregulation of the AIM2 DNA sensor links innate immunity with cell migration to promote epithelial tumourigenesis. Gut. 2022; 71: 1515–1531.

[22] Farshchian M, Nissinen L, Siljamäki E, Riihilä P, Piipponen M, Kivisaari A, *et al*. Tumor cell-specific AIM2 regulates growth and invasion of cutaneous squamous cell carcinoma. Oncotarget. 2017; 8: 45825–45836.

[23] So D, Shin H, Kim J, Lee M, Myeong J, Chun Y, *et al*. Cervical cancer is addicted to SIRT1 disarming the AIM2 antiviral defense. Oncogene. 2018; 37: 5191–5204.

[24] Hsu PC, Chao TK, Chou YC, Yu MH, Wang YC, Lin YH, *et al*. AIM2 inflammasome in tumor cells as a biomarker for predicting the treatment response to antiangiogenic therapy in epithelial ovarian cancer patients. Journal of Clinical Medicine. 2021; 10: 4529.

[25] Tschopp J, Martinon F, Burns K. NALPs: a novel protein family involved in inflammation. Nature Reviews Molecular Cell Biology. 2003; 4: 95–104.

[26] Kinoshita T, Wang Y, Hasegawa M, Imamura R, Suda T. PYPAF3, a PYRIN-containing APAF-1-like protein, is a feedback regulator of caspase-1-dependent interleukin-1beta secretion. Journal of Biological Chemistry. 2005; 280: 21720–21725.

[27] Li B, Qi Z, He D, Chen Z, Liu J, Wong M, *et al*. NLRP7 deubiquitination by USP10 promotes tumor progression and tumor-associated macrophage polarization in colorectal cancer. Journal of Experimental & Clinical Cancer Research. 2021; 40: 126.

[28] Ohno S, Kinoshita T, Ohno Y, Minamoto T, Suzuki N, Inoue M, *et al*. Expression of NLRP7 (PYPAF3, NALP7) protein in endometrial cancer tissues. Anticancer Research. 2008; 28: 2493–2497.

[29] Reynaud D, Abi Nahed R, Lemaitre N, Bolze PA, Traboulsi W, Sergent F, *et al*. NLRP7 promotes choriocarcinoma growth and progression through the establishment of an immunosuppressive microenvironment. Cancers. 2021; 13: 2999.

[30] Šutić M, Motzek A, Bubanović G, Linke M, Sabol I, Vugrek O, *et al*. Promoter methylation status of ASC/TMS1/PYCARD is associated with decreased overall survival and TNM status in patients with early stage non-small cell lung cancer (NSCLC). Translational Lung Cancer Research. 2019; 8: 1000–1015.

[31] Terasawa K, Sagae S, Toyota M, Tsukada K, Ogi K, Satoh A, *et al*. Epigenetic inactivation of TMS1/ASC in ovarian cancer. Clinical Cancer Research. 2004; 10: 2000–2006.

[32] Collard RL, Harya NS, Monzon FA, Maier CE, O'Keefe DS. Methylation

of the ASC gene promoter is associated with aggressive prostate cancer. The Prostate. 2006; 66: 687–695.

[33] Virmani A, Rathi A, Sugio K, Sathyanarayana UG, Toyooka S, Kischel FC, *et al*. Aberrant methylation ofTMS1 in small cell, non small cell lung cancer and breast cancer. International Journal of Cancer. 2003; 106: 198–204.

[34] Liang A, Zhong S, Xi B, Zhou C, Jiang X, Zhu R, *et al*. High expression of PYCARD is an independent predictor of unfavorable prognosis and chemotherapy resistance in glioma. Annals of Translational Medicine. 2021; 9: 986.

[35] Wang Z, Ni F, Yu F, Cui Z, Zhu X, Chen J. Prognostic significance of mRNA expression of CASPs in gastric cancer. Oncology Letters. 2019; 18: 4535–4554.

[36] Zhou Y, Dai W, Wang H, Pan H, Wang Q. Long non-coding RNA CASP5 promotes the malignant phenotypes of human glioblastoma multiforme. Biochemical and Biophysical Research Communications. 2018; 500: 966–972.

[37] Babas E, Ekonomopoulou MT, Karapidaki I, Doxakis A, Betsas G, Iakovidou-Kritsi Z. Indication of participation of caspase-2 and caspase-5 in mechanisms of human cervical malignancy. International Journal of Gynecological Cancer. 2010; 20: 1381–1385.

[38] Zhang Y, He R, Lei X, Mao L, Jiang P, Ni C, *et al*. A novel pyroptosis-related signature for predicting prognosis and indicating immune microenvironment features in osteosarcoma. Frontiers in Genetics. 2021; 12: 780780.

[39] Sha J, Du J, Yang J, Hu X, Li L. Changes of serum levels of tumor necrosis factor (TNF-α) and soluble interleukin-2 receptor (SIL 2R) in patients with cervical cancer and their clinical significance. American Journal of Translational Research. 2021; 13: 6599–6604.

[40] Behboodi N, Farazestanian M, Rastgar-Moghadam A, Mehramiz M, Karimi E, Rajabian M, *et al*. Association of a variant in the tumor necrosis factor alpha gene with risk of cervical cancer. Molecular Biology Reports. 2021; 48: 1433–1437.

How to cite this article: Dan Li, Zhihua Du, Hualin Song, Rongjuan Li, Changhui Han, Xiao Wang, *et al*. A novel pyroptosis-related gene signature for predicting the prognosis of cervical cancer. European Journal of Gynaecological Oncology. 2024; 45(2): 88-99. doi: 10.22514/ejgo.2024.031.